albite–crossite–acmite schists. Within these veins, jadeite is white with only a faint green tint developing along the vein contact. Earlier generations of green fibrous jadeite associated with albite are developed within the schists containing veins of white jadeite. Green jadeite also forms in pod-like bodies where it commonly exhibits cataclastic deformation and is healed by intersecting veins of white jadeite.

TABLE 1

Chemical analyses and optical properties of the Clear Creek Jd-rich pyroxenes, with atomic ratios

	1	2	3
SiO_2	59·38	59·06	56·54
Al_2O_3	25·82	24·62	18·38
TiO_2	0·04	0·08	0·44
Fe_2O_3	0·45	0·41	5·67
FeO	trace	0·18	1·05
MnO	nil	0·03	0·10
MgO	0·12	0·17	1·44
CaO	0·13	0·35	2·69
Na_2O	13·40	14·95	13·00
K_2O	0·02	0·01	0·03
H_2O^+	0·22	0·07	0·20
H_2O^-	0·16	0·03	0·05
Li_2O	—	nil	0·01
Cr_2O_3	0·01	—	—
TOTAL	99·75	99·96	99·60
S.G.	3·34 ± 0·006	—	—
α	1·654	1·654	1·679
β	1·657	1·656	1·681
γ	1·666	1·666	1·685
Biref.	0·012	0·012	0·006
$2V_z$ (+)	70° ± 2°	70° ± 2°	64° ± 2°
$Z \wedge c$	34° ± 1°	35° ± 1°	38° ± 1°
Disp.	none	none	$r > v$ strong
Jd	96·5	97·6	74·3
Ac	2·4	1·0	15·1
Di	1·1	0·9	7·5
He	—	0·5	3·2

Metal atoms to 6 (O)

	1			2			3		
Si	1·999	1·999	Z	1·997	1·997	Z	1·981	2·000	Z
Al	—			—			0·019		
Al	1·024	1·042	X	0·980	1·006	X	0·740	1·004	X
Ti	0·011			0·002			0·011		
Fe^{3+}	0·011			0·010			0·146		
Fe^{2+}	—			0·005			0·030		
Mn	—			0·001			0·003		
Mg	0·006			0·008			0·074		
Ca	0·005	0·879	Y	0·012	0·990	Y	0·101	0·984	Y
Na	0·873			0·978			0·882		
K	0·001			—			0·001		
		1·921			1·996			1·988	

1. White jadeite from veins (54-RGC-58) in albite-green jadeite schist from tectonic inclusions (see Fig. 5), Clear Creek, New Idria District, California (Locality No. 2, Fig. 2). Analyst: W. H. Herdsman, Glasgow, Scotland. Na_2O value is apparently in error as calculation of the formula to 6 (O) reveals a large discrepancy between Z group and the Σ (XY) groups.
2. White jadeite (J31–14) Clear Creek, New Idria District, California (Locality No. 1, Fig. 2). Collected by H. S. Yoder jr. Analysed sample loaned to the author by G. S. Switzer, U.S. National Museum. Analyst: Eileen H. Oslund, Univ. of Minnesota.
3. Green jadeite (J28–7) Clear Creek, New Idria District, California (Locality No. 1, Fig. 2). Collected by H. S. Yoder jr. Analysed sample loaned to the author by G. S. Switzer, U.S. National Museum. Analyst: Eileen H. Oslund, Univ. of Minnesota.

X-ray and optical determinations were made on splits of the analysed samples.

Two analyses of the white-vein jadeite and one of the green jadeite are given in Table 1. White-vein jadeite is very nearly pure Jd ($NaAlSi_2O_6$) whereas the green jadeite contains some Ac ($NaFe^{3+}Si_2O_6$), Di ($CaMgSi_2O_6$), and He ($CaFe^{2+}Si_2O_6$). Calculations of these analyses to the components Jd, Ac, Di, and He were made following the system used by Hess (1949). A chemical comparison of the Clear Creek jadeite with other jadeites and related jadeitic pyroxenes is shown in Fig. 3. From this comparison it can be seen that many of the pyroxenes referred to as jadeite may contain considerable amounts of the

(From *The American Mineralogist*, Vol. **51**: pp. 956-975, 1966)

THE CRYSTAL STRUCTURE OF JADEITE, $NaAlSi_2O_6$

C. T. PREWITT AND CHARLES W. BURNHAM

Papers from the
GEOPHYSICAL LABORATORY
Carnegie Institution of Washington
No. 1474

THE CRYSTAL STRUCTURE OF JADEITE, $NaAlSi_2O_6$

C. T. PREWITT, *Central Research Department*,[1] *E. I. du Pont de Nemours and Company, Experimental Station, Wilmington, Delaware*

AND

CHARLES W. BURNHAM,[2] *Geophysical Laboratory, Carnegie Institution of Washington, Washington, D. C.*

ABSTRACT

The crystal structure of naturally occurring pure jadeite has been refined by least-squares methods using single-crystal x-ray intensity data obtained by counter-diffractometer techniques. This jadeite is monoclinic, space group $C2/c$, with cell dimensions $a=9.418$ Å, $b=8.562$ Å, $c=5.219$ Å, and $\beta=107.58°$. The structure is similar to that of the pyroxene diopside and contains parallel sheets of octahedrally coordinated aluminum and 8-coordinated sodium polyhedra connected by silicate chains running parallel to the c axis. The mean cation-oxygen distances are Si-O = 1.623 Å, Al-O = 1.928 Å, and Na-O = 2.469 Å.

INTRODUCTION

Nearly forty years have passed since the crystal structure of diopside ($CaMgSi_2O_6$) was solved by Warren and Bragg (1928). Since then very little structural work has been done on the pyroxene minerals, and no modern refinements have been reported on structures of the diopside type. This investigation has been undertaken in order to provide precise information for the crystal structure of jadeite ($NaAlSi_2O_6$), a compound with the diopside structure.

Jadeite is particularly interesting because it has often been referred to as a "pressure mineral," that is, a phase whose formation is favored by high pressure. It is a chemical component of the mineral omphacite and is, as a consequence, of considerable importance to geophysics and petrology. In addition, the availability of detailed structural data on jadeite and other similar pyroxenes is critical to a complete understanding of the phase-equilibrium relations within this important group of rock-forming silicates.

PREVIOUS WORK

Wyckoff *et al.* (1925) recognized that powder diffraction diagrams of jadeite and diopside are similar. Warren and Bragg (1928) solved the structure of diopside, and subsequently Warren and Biscoe (1931) predicted that jadeite and diopside have the same structure. Morimoto *et al.* (1960) determined and refined the structures of the monoclinic pyroxenes clinoenstatite ($MgSiO_3$) and pigenoite ($Ca_{0.10}Mg_{0.34}Fe_{0.56}$-

[1] Contribution No. 1162.

[2] Present address: Department of Geological Sciences, Harvard University, Cambridge, Mass.

SiO_3). Although these are clinopyroxenes, their structures and space groups are different from those of diopside.

SPECIMEN DESCRIPTION

Crystals of jadeite were obtained from a specimen supplied by Dr. H. S. Yoder, Jr. (No. 184). The material is from the Santa Rita Peak area of the New Idria Peak District, California, and occurs in veinlets cutting across albite-crossite-acmite schists. Descriptions of the locality are given by Yoder and Chesterman (1951) and Coleman (1961). The optics of this material were checked by Professor C. E. Tilley and found to be essentially the same as those reported for Coleman's sample J31-14.

TABLE 1. ELECTRON MICROPROBE ANALYSIS OF SANTA RITA PEAK JADEITE

Oxide	Weight per cent		Ion	Number of atoms	
	Blue fluor.	Turquoise fluor.		Blue fluor.	Turquoise fluor.
SiO_2	58.07	57.68	Si^{4+}	1.967	1.953
TiO_2	0.05–0.010	0.0–0.03	Ti^{4+}	0.001–0.003	0.0–0.001
Al_2O_3	24.89	24.59	Al^{3+}	0.994	0.981
Fe_2O_3	0.43	0.50	Fe^{3+}	0.011	0.013
MgO	0.01	0.46	Mg^{2+}	0.001	0.023
MnO	—	0.03–0.05	Mn^{2+}	—	0.001
CaO	0.14	0.87	Ca^{2+}	0.005	0.031
Na_2O	16.62	16.44	Na^{1+}	1.092	1.080
K_2O	0.04	0.02	K^{1+}	0.002	0.001
	100.25–100.30	100.62–100.67			
			O^{2-}	6.000	6.000

Professor J. V. Smith kindly agreed to examine our specimen using the electron microprobe. He found that two compositional variants could be distinguished by this technique; one that fluoresced blue, the other green. The analyses of bulk material of both types, uncorrected for absorption and atomic number, are listed in Table 1. Electron microprobe examination of the same crystal used for x-ray intensity measurements showed that it fluoresced blue with a tendency toward green at either end. Considering the variation of composition of this crystal, assuming the iron to be present as Fe^{3+}, and neglecting the cations present in amounts less

than 0.01 atom per 6 oxygen atoms, the best approximation to the chemical formula is $(Na^{1+}_{0.98}Ca^{2+}_{0.02})(Al^{3+}_{0.99}Mg^{2+}_{0.01})(Si^{4+}_{1.99}Fe^{3+}_{0.01})O_6$. This, then, is an unusually pure jadeite specimen, and one could hardly hope to find much better material occurring naturally.

Unit Cell and Space Group

Some difficulty was encountered in finding a suitable single crystal for intensity measurement. Many of the crystals we examined showed streaked spots parallel to the rotation axis on c-axis Weissenberg films, indicating that the crystals were actually made up of bundles of crystallites slightly misoriented with respect to each other around c. A small,

Table 2. Unit-Cell Dimensions of Santa Rita Peak Jadeite, and, for Comparison, Synthetic Jadeite and Synthetic Diopside

	Jadeite, Santa Rita Peak	Jadeite, synthetic (Frondel and Klein, 1965)	Diopside, synthetic (Clark *et al.*, 1962)
a, Å	9.418±0.001	9.418±0.006	9.745±0.001
b, Å	8.562±0.002	8.563±0.004	8.925±0.001
c, Å	5.219±0.001	5.211±0.006	5.248±0.001
β, deg.	107.58±0.01	107.57 ±0.05	105.87 ±0.01
V, Å^3	401.20 ±0.15	400.7 ±0.6	439.08 ±0.07

apparently homogeneous crystal with approximate dimensions 0.04 ×0.08×0.22 mm. that exhibited no such streaking was finally selected for intensity measurement.

From x-ray photographs we could detect no deviations from space group $C2/c$ such as have been observed on photographs of spodumene and omphacite (D. R. Peacor, D. E. Appleman, and J. R. Clark, personal communications).

The unit-cell dimensions were determined by least-squares refinement of 76 measurements from Straumanis-mounted precision back-reflection Weissenberg photographs. The refinement procedure includes allowance for systematic errors due to specimen absorption, film shinkage, and camera eccentricity (Burnham, 1962). The results are listed in Table 2 where they are compared with refined powder diffraction data for pure synthetic jadeite and pure synthetic diopside. We have followed the conventional setting of a right-handed coordinate system with the positive a and c axes enclosing an obtuse angle, β. Although several authors have used this setting (see, for example, Deer, *et al.* 1963, p. 43), the unconventional setting of Warren and Bragg (1928) with β acute still persists in

the literature (see, for example, Kuno and Hess, 1953). We strongly recommend that the conventional setting with β obtuse be adopted by all workers, especially those listing indexed powder diffraction data.

Intensity Measurement and Structure Refinement

Diffraction intensities were measured using an equi-inclination Weissenberg diffractometer, a scintillation detector, and pulse height analyzer set to pass 90 per cent of the diffracted Ni-filtered CuKα radiation. Of the 362 *hkl* reflections measured, 14 had intensities less than the minimum observable value and were assigned values equal to $I_{min.}/3$ (Hamilton, 1955); these "unobserved" intensities were not used during the refinement procedure. Integrated intensities were corrected for absorption, using a numerical integration technique (Burnham, 1965a), and for Lorentz and polarization effects.

Structure refinement was carried out on an IBM 7094 computer using a modified version of a full matrix least-squares program written by Prewitt (1962). The modified program uses an analytic expression for scattering curves; some technical details concerning this representation are given in the Appendix. The refinement was carried to convergence using scattering curves for fully ionized atoms.

Refinement was initiated using the Warren and Bragg (1928) atomic coordinates of diopside transformed to the conventional unit cell, and using individual isotropic temperature factors of 0.6 for oxygen atoms, 0.4 for Si, 0.4 for Al, and 0.75 for Na. Calculated structure factors were scaled to the observed ones using one refineable scale factor, and observations were weighted in inverse proportion to their variance computed from consideration of counting statistics. After several cycles of least-squares during which atomic coordinates, isotropic temperature factors, and one scale factor were varied, the R value $(\sum||F_o|-|F_c||/\sum|F_o|)$ for 430 observations reached 0.045. Temperature factors were then converted to anisotropic form, and four cycles of refinement, varying the scale factor, atomic coordinates, and anisotropic temperature factors, further reduced the R value to 0.040.

At this point analysis of the data revealed an apparent systematic error that we attributed to extinction. The observed intensities were corrected for extinction according to Zacharaisen's (1963) method, using

$$I_{corr.} = \frac{I_{obs.}}{(1 - tI_{obs.})}$$

where $t = 1\times10^{-6}$; this value was obtained by comparison of observed and calculated intensities from the last previous cycle of refinement.

Apparent divergence during the first refinement cycle carried out with

the corrected data led to adoption of a new weighting scheme (Cruickshank, 1960), in which the variance of the observed structure factor, $\sigma^2_{|Fo|}$, is given by

$$\sigma^2|F_o| = \left(2F_{\text{min.}} + F_o + \frac{2}{F_{\text{max.}}} F_o^2\right)$$

Three cycles of coordinate, anisotropic temperature factor, and scale factor refinement resulted in convergence to an R value for all observations (including those with $|F_o| < |F_o|_{\text{min.}}$) of 0.037.

One of the important purposes of precise refinements of silicate structures is the determination of atomic thermal models. If all systematic errors in the data are taken into account, and if the chemical composition is known, analysis of apparent atomic vibration ellipsoids can yield indications of the presence or absence of disorder, either substitutional or positional. Such analysis depends to a large extent on reliable knowledge of expected thermal models for atoms in pure, ordered structures. Our knowledge at present is neither reliable nor extensive, chiefly because the temperature factors determined by least-squares refinement are strongly affected by systematic errors due to absorption, extinction, etc. Since our specimen of jadeite was shown to be quite pure, and since we had applied a precise absorption correction and made an attempt to correct for extinction, we felt it would be worthwhile to test the effects on temperature factors of anomalous dispersion corrections and variations of the ionization states of the atoms.

Additional refinement cycles were carried out under the following three conditions:

(*a*) anomalous dispersion corrections, both real and imaginary, applied to fully ionized atoms; (*b*) anomalous dispersion corrections applied to neutral atoms; (*c*) substitution of the scattering curve of Al^{3+} for that of Si^{4+}, anomalous dispersion included.

Some details of the method for correcting for anomalous dispersion are given in the Appendix. For CuKα radiation the anomalous dispersion corrections are small; the largest is the imaginary term for Si (0.4 electron). Throughout these tests the atomic coordinates either remained unchanged or, in some cases, changed by less than 1σ. The temperature factors did change, as expected, and when $f_{Al}{}^{3+}$ was substituted for $f_{Si}{}^{4+}$, β_{33} for that atom immediately became negative. Table 3 lists the atomic coordinates and equivalent isotropic temperature factors from the final stage of refinement with no anomalous dispersion corrections, and compares them with the results from cases *a* and *b* above. Equivalent isotropic temperature factors were computed according to (Hamilton, 1959)

$$B_{\text{equiv.}} = \frac{4}{3}\sum_i \sum_j \beta_{ij}\mathbf{a}_i \cdot \mathbf{a}_j$$

where the $\mathbf{a}_i$ are the axial vectors of the unit cell.

Application of anomalous dispersion corrections increased the equivalent B's for all cations, with that for Si^{4+} being the most significant; and decreased the B's for oxygen atoms by about 0.05. The effect on cation B's of changing ionization state is insignificant, whereas the effect on oxygen atoms is just about equal in magnitude but of opposite sign to that of the anomalous dispersion correction.

Comparison of apparent vibration ellipsoids, both as to magnitude and

TABLE 3. COMPARISON OF ATOMIC COORDINATES AND EQUIVLAENT ISOTROPIC TEMPERATURE FACTORS OBTAINED FROM DIFFERING REFINEMENT CONDITIONS AS FOLLOWS: COLUMN A, FULLY IONIZED ATOMS, ANOMALOUS DISPERSION NOT INCLUDED; COLUMN B, FULLY IONIZED ATOMS, ANOMALOUS DISPERSION INCLUDED; COLUMN C, NEUTRAL ATOMS, ANOMALOUS DISPERSION INCLUDED

Atom, parameter	A	B	C
Na, y	0.3009	0.3009	0.3010
B	0.90	0.95	0.96
Al, y	0.0940	0.0940	0.0940
B	0.36	0.40	0.42
Si, x	0.2906	0.2906	0.2906
y	0.0934	0.0934	0.0934
z	0.2277	0.2277	0.2278
B	0.32	0.41	0.39
O_1, x	0.1090	0.1090	0.1089
y	0.0763	0.0763	0.0764
z	0.1275	0.1275	0.1277
B	0.41	0.36	0.43
O_2, x	0.3608	0.3608	0.3610
y	0.2630	0.2630	0.2629
z	0.2929	0.2929	0.2933
B	0.53	0.48	0.55
O_3, x	0.3533	0.3533	0.3535
y	0.0070	0.0070	0.0070
z	0.0058	0.0058	0.0060
B	0.53	0.48	0.54

orientation, shows that the only significant differences occur between the Si ellipsoids determined with and without anomalous dispersion effects. When anomalous dispersion is included, the rms displacements of Si along the principal axes increase by 0.009 Å, which is just over 2σ. The orientation of the ellipsoid does not change. For all other atoms the changes in rms displacements were $\leqq 1\sigma$, and there were no changes in ellipsoid orientations.

These tests indicate that, at the level of precision this refinement represents, the selection of ionization state is arbitrary and will not significantly influence either atomic coordinates or thermal models. The influence of anomalous dispersion corrections is also negligible if the correction terms are not greater than 0.1–0.2 electron. If they are larger, their effect should be taken into account during refinement to obtain correct apparent thermal models.

As a test of the influence of weighting scheme on these refinement results, the last three cycles of least squares were repeated using the original weighting scheme based on counting statistics (see Appendix). These cycles included anomalous dispersion corrections and assumed ionized atoms. The final results are identical with those obtained with the Cruickshank-type weighting scheme under the same conditions.

We have selected the parameters resulting from refinement with scattering curves for ionized atoms and including anomalous dispersion corrections as the final, refined values. These are listed with their standard deviations in Table 4. The observed and calculated structure factors are listed in Table 5. The observed values contain absorption, Lorentz and polarization, and extinction corrections and have been reduced to the absolute scale of the calculated values by division by the least-squares scale factor. The calculated values contain the correction for both real and imaginary components of anomalous dispersion (see Appendix), hence are unsigned.

Discussion of the Structure

Coordination polyhedra. Figure 1 is a diagram of a polyhedral model for jadeite. The model consists of parallel sheets of aluminum-oxygen and sodium-oxygen polyhedra connected by silicate chains running in the *c* direction. The Al is octahedrally coordinated by oxygen, and Na is coordinated by eight oxygen atoms in a polyhedron which is intermediate between a cube and a square antiprism.

Some confusion exists in the literature concerning the coordination of Ca in the diopside structure (or Na in jadeite) and the sharing of oxygens between the Ca polyhedron and the silicate chains. For example, Warren and Bragg (1928) state that Ca in diopside is surrounded by six

Table 4. Final Atomic Coordinates, Anisotropic Temperature Factors, and Equivalent Isotropic Temperature Factors for Atoms in Jadeite. Standard Deviations, σ, Given in Parentheses

Atom (equipoint)		x	y	z	β_{11}	β_{22}	β_{33}	β_{12}	β_{13}	β_{23}	B (equiv.)
Na	(4e)	0	0.3009 (2)	1/4	0.0035 (2)	0.0026 (3)	0.0074 (8)	0	−0.0002 (3)	0	0.95
Al	(4e)	0	0.0940 (1)	3/4	0.0013 (2)	0.0015 (2)	0.0035 (6)	0	0.0005 (3)	0	0.40
Si	(8f)	0.2906 (1)	0.0934 (1)	0.2277 (2)	0.0011 (1)	0.0017 (2)	0.0036 (5)	0.0000 (1)	0.0006 (2)	−0.0001 (2)	0.41
O_1	(8f)	0.1090 (2)	0.0763 (3)	0.1275 (4)	0.0004 (3)	0.0020 (3)	0.0032 (9)	−0.0004 (2)	0.0000 (4)	−0.0007 (4)	0.36
O_2	(8f)	0.3608 (2)	0.2630 (3)	0.2929 (4)	0.0010 (3)	0.0020 (3)	0.0047 (9)	−0.0004 (2)	0.0000 (4)	0.0002 (4)	0.48
O_3	(8f)	0.3533 (2)	0.0070 (3)	0.0058 (4)	0.0013 (3)	0.0022 (3)	0.0041 (10)	−0.0003 (2)	0.0009 (4)	0.0000 (4)	0.49

TABLE 5. OBSERVED AND CALCULATED STRUCTURE FACTORS.
Observed values marked with an asterisk represent statistical assignments to reflections with intensities less than the minimum observable.

H	K	L	F(OBS)	F(CAL)	H	K	L	F(OBS)	F(CAL)
2	0	0	15.13	8.29	-7	5	1	9.02	7.76
4	0	0	14.98	12.02	-8	5	1	18.60	17.89
6	0	0	66.52	68.07	-3	5	1	8.94	8.52
8	0	0	50.43	53.40	-1	5	1	25.78	25.83
10	0	0	52.74	52.04	1	5	1	2.78	5.33
1	1	0	14.21	13.71	3	5	1	24.51	23.30
3	1	0	88.97	86.20	5	5	1	20.82	20.80
5	1	0	58.59	61.59	7	5	1	14.59	13.09
7	1	0	41.15	44.24	-8	6	1	9.64	9.69
9	1	0	6.06	6.02	-6	6	1	16.19	15.07
0	2	0	56.37	52.92	-4	6	1	16.71	16.26
2	2	0	41.46	38.66	-2	6	1	14.16	15.26
4	2	0	14.02	13.61	0	6	1	36.49	37.53
6	2	0	10.04	10.47	2	6	1	9.71	9.01
8	2	0	10.77	10.26	4	6	1	9.82	10.28
10	2	0	16.17	16.31	6	6	1	4.22	5.64
1	3	0	9.16	8.20	-7	7	1	2.71	1.09
3	3	0	48.88	50.01	-5	7	1	69.38	71.28
5	3	0	26.13	26.15	-3	7	1	16.57	15.99
7	3	0	24.40	24.47	-1	7	1	49.17	51.01
9	3	0	21.38	21.33	1	7	1	50.74	50.69
0	4	0	4.82	2.30	3	7	1	4.24	4.72
2	4	0	8.22	8.60	5	7	1	49.39	48.70
4	4	0	75.55	77.03	-6	8	1	22.81	22.34
6	4	0	19.26	18.55	-4	8	1	8.34	8.66
8	4	0	18.81	19.52	-2	8	1	73.70	74.22
1	5	0	71.73	69.19	0	8	1	14.52	14.51
3	5	0	67.02	70.75	2	8	1	58.06	59.03
5	5	0	23.56	23.05	4	8	1	5.33	3.89
7	5	0	90.68	91.53	-5	9	1	47.68	47.34
9	5	0	4.25	3.82	-3	9	1	4.62	3.22
0	6	0	94.86	97.14	-1	9	1	6.88	6.33
2	6	0	23.80	22.57	1	9	1	11.02	10.47
4	6	0	26.05	24.64	3	9	1	11.32	11.26
6	6	0	1.27*	0.78	0	10	1	22.43	26.05
8	6	0	8.55	8.62	-10	0	2	65.84	64.74
1	7	0	25.81	25.09	-8	0	2	17.59	17.29
3	7	0	15.81	14.32	-6	0	2	87.44	91.71
5	7	0	45.90	45.10	-4	0	2	72.26	72.46
7	7	0	46.55	45.24	-2	0	2	47.45	43.95
0	8	0	1.68*	2.32	2	0	2	51.90	52.23
2	8	0	17.20	20.72	4	0	2	96.50	105.95
4	8	0	23.50	24.08	6	0	2	6.27	5.33
6	8	0	11.11	10.99	8	0	2	18.31	19.67
1	9	0	3.95	4.48	-11	1	2	9.55	9.72
3	9	0	27.14	28.89	-9	1	2	13.00	15.04
0	10	0	66.08	65.66	-7	1	2	100.39	103.79
-7	1	1	17.06	18.91	-5	1	2	29.15	30.35
-5	1	1	33.25	34.31	-3	1	2	6.60	5.46
-3	1	1	68.95	70.40	-1	1	2	12.02	10.96
-1	1	1	91.07	88.41	1	1	2	76.67	74.87
1	1	1	11.80	10.73	3	1	2	37.11	38.64
3	1	1	67.08	69.28	5	1	2	35.39	36.17
5	1	1	21.43	22.50	7	1	2	53.63	55.00
7	1	1	8.27	8.30	9	1	2	23.08	24.00
9	1	1	18.92	17.94	-10	2	2	39.88	38.93
10	2	1	17.60	17.51	-8	2	2	22.28	22.29
-8	2	1	43.18	42.85	-6	2	2	30.73	30.15
-6	2	1	34.13	35.68	-4	2	2	39.40	38.76
-4	2	1	48.08	49.89	-2	2	2	13.21	13.41
-2	2	1	126.32	125.53	0	2	2	61.27	58.82
0	2	1	42.13	38.05	2	2	2	20.96	21.31
2	2	1	92.40	89.44	4	2	2	61.77	61.32
4	2	1	10.79	9.50	6	2	2	32.60	32.80
8	2	1	46.53	45.91	8	2	2	32.69	34.22
-9	3	1	51.16	48.22	-11	3	2	2.13	5.48
-7	3	1	51.47	51.75	-9	3	2	6.43	5.27
-5	3	1	112.19	118.44	-7	3	2	18.04	18.04
-3	3	1	73.33	70.92	-5	3	2	22.94	22.74
-1	3	1	64.27	63.23	-3	3	2	24.95	23.15
1	3	1	22.32	20.54	-1	3	2	39.13	39.33
3	3	1	21.46	20.55	1	3	2	32.49	32.78
5	3	1	123.47	131.36	3	3	2	9.59	9.09
7	3	1	22.21	22.84	5	3	2	17.23	17.58
9	3	1	43.45	42.07	7	3	2	9.74	8.60
-10	4	1	24.00	21.81	-10	4	2	34.61	33.29
-8	4	1	1.61*	0.76	-8	4	2	5.82	5.60
-6	4	1	11.44	10.56	-6	4	2	26.73	26.92
-4	4	1	16.39	15.54	-4	4	2	16.60	16.27
-2	4	1	53.62	52.37	-2	4	2	19.26	18.76
0	4	1	92.58	90.33	0	4	2	62.62	63.35
2	4	1	20.96	20.38	2	4	2	34.07	33.01
4	4	1	12.55	13.78	4	4	2	43.43	45.65
6	4	1	21.66	21.16	6	4	2	5.95	5.68
8	4	1	11.05	9.69	8	4	2	7.12	6.08
-9	5	1	2.49	0.41	-9	5	2	19.14	18.38

TABLE 5—(continued)

H	K	L	F(OBS)	F(CAL)	H	K	L	F(OBS)	F(CAL)
-7	5	2	69.75	68.11	-4	8	3	14.04	14.14
-5	5	2	8.42	8.62	-2	8	3	47.19	46.36
-3	5	2	105.72	115.02	0	8	3	1.02*	0.92
-1	5	2	7.38	5.88	2	8	3	67.49	66.50
1	5	2	37.67	37.77	-10	0	4	30.09	27.65
3	5	2	100.45	104.18	-8	0	4	15.86	16.29
5	5	2	4.41	1.64	-6	0	4	106.97	113.55
7	5	2	42.35	40.09	-4	0	4	43.47	44.50
-8	6	2	7.70	7.05	-2	0	4	94.89	103.74
-6	6	2	64.22	64.19	0	0	4	1.16*	1.19
-4	6	2	3.88	4.44	2	0	4	64.26	65.37
-2	6	2	57.31	58.19	4	0	4	15.30	14.87
0	6	2	99.00	103.32	6	0	4	5.38	4.11
2	6	2	10.94	10.49	-9	1	4	5.38	5.67
4	6	2	24.98	24.61	-7	1	4	27.62	27.33
6	6	2	4.94	2.50	-5	1	4	10.21	10.51
-7	7	2	20.17	20.77	-3	1	4	94.62	91.40
-5	7	2	19.91	19.06	-1	1	4	46.61	46.83
-3	7	2	14.42	15.08	1	1	4	2.52	2.37
-1	7	2	34.10	33.07	3	1	4	44.77	44.83
1	7	2	10.55	9.48	5	1	4	4.22	3.66
3	7	2	35.58	34.80	-10	2	4	4.19	5.67
5	7	2	27.33	26.86	-8	2	4	13.57	14.60
-6	8	2	18.34	17.92	-6	2	4	11.20	10.81
-4	8	2	1.15*	2.23	-4	2	4	7.86	7.54
-2	8	2	2.34	2.27	-2	2	4	7.75	8.41
0	8	2	16.91	16.84	0	2	4	10.72	11.29
2	8	2	14.62	14.66	2	2	4	40.04	41.89
4	8	2	12.93	12.78	4	2	4	17.80	18.37
-9	9	2	9.66	9.70	-9	3	4	15.65	15.56
-7	9	2	7.72	7.09	-7	3	4	18.79	17.72
-5	9	2	2.54	2.07	-5	3	4	16.99	16.13
-3	9	2	21.56	20.42	-3	3	4	23.75	24.02
-1	9	2	2.54	2.07	-1	3	4	7.42	7.45
-9	1	3	3.42	2.86	1	3	4	14.21	12.63
-7	1	3	16.53	17.46	3	3	4	21.43	21.23
-5	1	3	31.62	31.85	5	3	4	18.88	19.43
-3	1	3	64.43	64.75	-8	4	4	20.48	20.64
-1	1	3	26.23	25.53	-6	4	4	3.15	2.77
1	1	3	16.99	17.09	-4	4	4	33.84	33.21
3	1	3	29.99	31.01	-2	4	4	17.07	17.28
5	1	3	3.48	3.20	0	4	4	10.17	9.83
7	1	3	10.92	9.92	2	4	4	33.71	33.15
-10	2	3	6.16	5.87	4	4	4	64.47	62.88
-8	2	3	62.14	65.13	-7	5	4	69.06	68.92
-6	2	3	1.27*	0.19	-5	5	4	1.06*	2.53
-4	2	3	21.10	22.81	-3	5	4	73.00	76.68
-2	2	3	99.63	98.69	-1	5	4	3.49	2.82
0	2	3	8.83	8.33	1	5	4	44.33	43.80
2	2	3	78.53	82.10	3	5	4	34.49	32.08
4	2	3	23.30	24.26	-6	6	4	42.18	41.31
6	2	3	47.56	48.35	-4	6	4	37.10	35.85
-9	3	3	62.73	61.65	-2	6	4	16.71	16.60
-7	3	3	36.29	37.49	0	6	4	26.40	25.26
-5	3	3	65.16	67.69	2	6	4	16.34	16.01
-3	3	3	18.56	17.34	-5	7	4	2.42	1.78
-1	3	3	107.06	106.88	-3	7	4	9.54	9.93
1	3	3	10.79	10.70	-1	7	4	24.91	23.96
3	3	3	5.59	3.35	1	7	4	13.91	13.24
5	3	3	68.45	69.42	-8	1	5	0.80*	2.56
7	3	3	10.56	10.60	-7	1	5	4.13	4.00
-8	4	3	30.11	29.86	-5	1	5	31.36	31.68
-6	4	3	37.98	38.67	-1	1	5	12.78	11.73
-4	4	3	12.30	12.29	1	1	5	7.84	7.92
-2	4	3	53.38	54.02	3	1	5	3.24	2.52
0	4	3	28.63	28.99	-6	2	5	5.01	4.26
2	4	3	18.31	19.21	-4	2	5	22.14	22.94
4	4	3	35.94	36.65	-2	2	5	34.05	33.27
6	4	3	20.32	20.43	0	2	5	7.63	5.36
-9	5	3	2.41	1.48	2	2	5	75.68	76.05
-7	5	3	1.25*	0.72	-7	3	5	3.89	4.78
-5	5	3	15.72	15.97	-5	3	5	44.70	44.40
-3	5	3	20.20	18.99	-3	3	5	21.44	21.57
-1	5	3	20.45	20.31	-1	3	5	78.05	77.90
1	5	3	25.75	24.56	1	3	5	8.46	8.96
3	5	3	13.15	12.66	-6	4	5	16.67	17.00
5	5	3	9.80	9.11	-4	4	5	6.35	6.15
-8	6	3	6.29	5.81	-2	4	5	8.20	8.15
-6	6	3	10.65	11.33	0	4	5	12.68	12.56
-4	6	3	1.17*	0.60	2	4	5	38.76	37.00
-2	6	3	5.34	3.25	-5	5	5	13.70	13.17
0	6	3	33.09	32.46	-3	5	5	20.90	21.74
2	6	3	14.52	14.14	-1	5	5	7.70	7.67
4	6	3	10.60	9.79	-4	6	5	2.91	0.76
-7	7	3	3.19	3.09	-2	6	5	10.59	11.87
-5	7	3	58.49	57.21	-2	0	6	27.01	27.11
-3	7	3	18.77	19.43	-5	1	6	17.12	16.83
-1	7	3	55.85	56.57	-1	1	6	7.10	6.66
1	7	3	28.81	29.38	-4	2	6	0.75*	2.77
3	7	3	6.29	4.18	-2	2	6	20.96	21.04

oxygens plus two "neutral" oxygens, each of which is also coordinated to two Si. Examination of Fig. 1 shows, however, that there are actually four oxygens surrounding Na that are also coordinated to two Si. In another example, Deer *et al.* (1963) state that only two of the eight oxygens

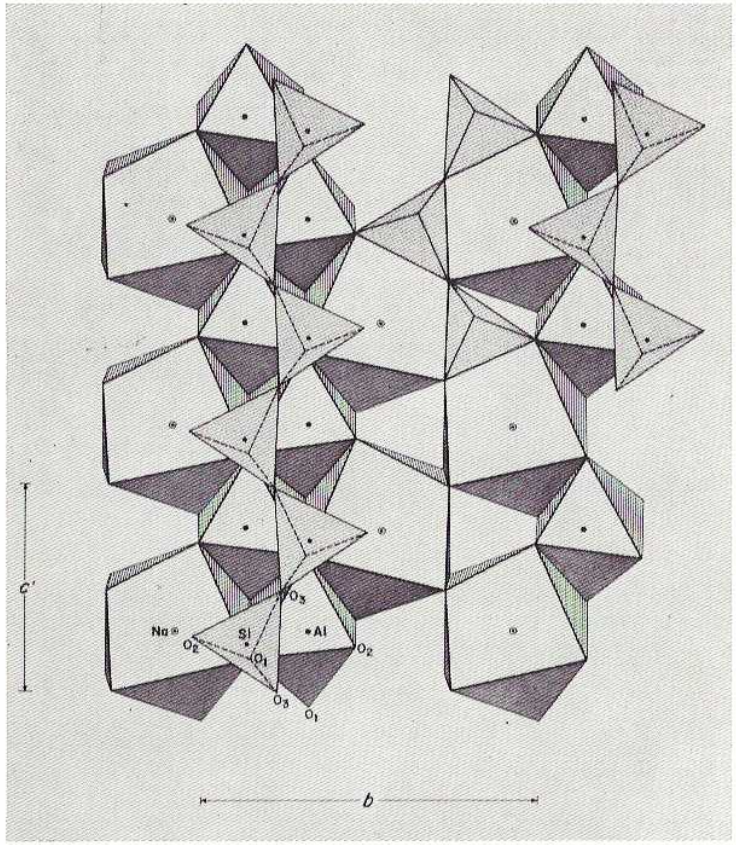

FIG. 1. Polyhydral model for jadeite projected along a direction about halfway between a and a*. Projection along a* would cause Si and O_1 to be nearly superimposed.

around Ca in diopside are also shared by neighboring tetrahedra. This statement is erroneous, since all the oxygen atoms in both diopside and jadeite are coordinated to at least one Si.

The coordination found for Na in jadeite is rather common among sodium-containing silicates. For example, in pectolite (Prewitt, 1965) and fluor-magnesio-richterite (Prewitt, 1964), Na has a similar coordination, as seen in Fig. 2. In pectolite the coordination is somewhat affected by the presence of hydrogen, but it is essentially the same as in other compounds.

Interatomic distances and interbond angles for jadeite are given in Tables 6 and 7. These were computed using the Busing *et al.* (1964)

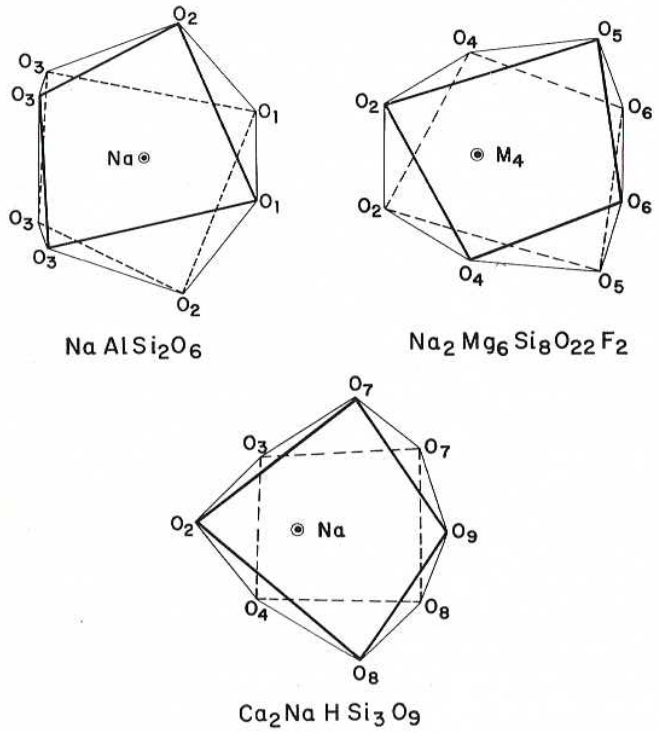

FIG. 2. Coordination polyhedra for Na in jadeite, fluor-magnesio-richterite, and pectolite.

program ORFFE and the atom coordinates of Table 4. The standard errors of both the cell parameters and the refined atom coordinates were used to compute the distance and angle errors.

All the coordination polyhedra in jadeite are distorted, partly because of extensive sharing of polyhedral elements and partly because the polyhedra are distorted so that the structure will fit together properly. The Si-O distances range from 1.590 to 1.637 Å, and the tetrahedral O-O distances range from 2.575 to 2.773 Å. The two shortest O-O distances,

O_2-O_3' (2.575 Å) and O_3-O_3' (2.612 Å), represent edges that are shared with the Na polyhedron.

The Al octahedra form "chains" parallel to the silicate chains by sharing a common edge with length 2.458 Å (O_1-O_1''). Two additional edges of each octahedron are shared with Na polyhedra to form the Al,Na polyhedral sheets. The edges shared with the Na polyhedra have lengths

TABLE 6. INTERATOMIC DISTANCES IN JADEITE

Atom pair	Distance, Å, $\pm\sigma$	Atom pair	Distance, Å, $\pm\sigma$
Si tetrahedron:		Al octahedron:	
Si-O_1	1.637±0.002	Al-O_1 (2)	1.933±0.002
Si-O_2	1.590±0.002	Al-O_2 (2)	1.856±0.002
Si-O_3	1.628±0.002	Al-O_1' (2)	1.996±0.002
Si-O_3'	1.636+0.002		
Mean Si-O	1.623	Mean Al-O	1.928
O_1-O_2	2.773±0.003	O_1-O_1' (2)	2.918±0.002
O_1-O_3	2.633±0.003	O_1-O_1'' (2)	2.458±0.004
O_1-O_3'	2.638±0.003	O_1-O_2 (2)	2.818±0.00
O_2-O_3	2.644±0.003	O_1-O_2' (2)	2.677±0.003
O_2-O_3'	2.575±0.003	O_1'-O_1''	2.726±0.004
O_3-O_3'	2.612±0.0004	O_2-O_2'	2.790±0.004
		O_1''-O_2 (2)	2.716±0.004
Mean O-O	2.646	Mean O-O	2.714
SiO_3^{2-} chain:			
Si-Si'	3.061±0.001	Al-Al' (across shared edge)	3.066±0.001
Na polyhedron:			
Na-O_1 (2)	2.357±0.003		
Na-O_2 (2)	2.413±0.002		
Na-O_3 (2)	2.363±0.003		
Na-O_3' (2)	2.741±0.002		
Mean Na-O	2.469		

of 2.818 Å—distances that show no apparent shortening due to sharing effects. The octahedral edge-sharing geometry may be compared with that in other structures by considering the following: The average Al-O distance to oxygen atoms forming the shared edge (there are two symmetry-related shared edges per octahedron, hence we need only examine the geometry of one) is 1.965 Å, the shared edge length is 2.458 Å, and the Al-Al separation is 3.066 Å. When these values are compared with similar ones for other octahedra, as has been done in discussing the structure of kyanite (Burham, 1963, Fig. 3), it is apparent that the average Al-O distance is longer than normal, the Al-Al separation is larger than normal, but the O-O distance along the shared edge is within the expected range. The electrostatic charge balance on O_1, which is coordinated to Si, two Al atoms, and Na, is $+\frac{1}{8}$ when computed with classic valences on cations. Thus, there is an immediate explanation for the long Al-O_1 distances (and the long Si-O_1 distance as well). The Al-Al separation is probably longer than expected because of the apparent weakness of shielding by the two "surplus-charged" oxygen atoms.

TABLE 7. INTERATOMIC ANGLES IN JADEITE

Atoms	Angle, degrees, $\pm\sigma$
Si tetrahedron:	
O_1-Si-O_2	118.5±0.1
O_1-Si-O_3	107.5±0.1
O_1-Si-O_3'	107.4±0.1
O_2-Si-O_3	110.5±0.1
O_2-Si-O_3'	105.9±0.1
O_3-Si-O_3'	106.3±0.1
SiO_3^{2-} chain:	
Si-O_3-Si'	139.3±0.1
O_3-O_3'-O_3''	174.7±0.2
Al octahedron:	
O_1-Al-O_1'	95.9±0.1
O_1-Al-O_1''	77.4±0.1
O_1-Al-O_2'	89.9±0.1
O_1'-Al-O_1''	86.2±0.1
O_2-Al-O_2'	97.5±0.2
O_1''-Al-O_2	89.6±0.1

The classic electrostatic charge balance (Pauling, 1960) fails on all oxygen atoms. On O_1 the balance is $+\frac{1}{8}$, on O_2 it is $-\frac{3}{8}$, and on O_3 it is $+\frac{1}{4}$. It is apparent from examining bond lengths that the standard charge distribution is not the correct one. As we have already seen, both the Al-O_1 and Si-O_1 distances are abnormally long, yet the shortest Na-O distance is to O_1. The chain-forming oxygen, O_3, is coordinated to two Si, at distances that differ by 0.008 Å ($=4\sigma$); and to one Na at 2.363 Å and another Na at 2.741 Å. This long distance must represent an extremely weak bond, and the effective coordination of O_3 is probably closer to 3 than 4. The distances from both Si and Al to O_2, the "charge-deficient" oxygen, are significantly shorter than average, as would be expected. The Na-O_2 distance, however, is apparently not affected—it is longer than Na-O_1 and one of the Na-O_3 distances.

Morimoto, Appleman, and Evans (1960) remarked on the similarity of the Si-Si distances in clinoenstatite, pigeonite, and diopside. The distance in all three structures is 3.05±0.02 Å, whereas in jadeite it is 3.061 Å. It may be that such fairly uniform distances are significant features of these compounds since 3.05 Å is about the smallest Si-Si distance reported for well-refined chain silicates. Several larger distances are known, however, including one of 3.17 Å in wollastonite (Buerger and Prewitt, 1961).

An unusual feature of the jadeite structure is the "straightness" of the silicate chain, as revealed by the O_3-O_3'-O_3'' angle of 174.7°. Although this angle has not generally been reported in pyroxene structure results, it is probably closer to 180° in jadeite than in any other pyroxenes that have been investigated in detail. In contrast to this, the Si-O_3-Si′ angle of 139.3 is close to the average Si-O-Si angle found in these structures.

Thermal models. The rms displacements and orientations of the principal axes of the thermal vibration ellipsoid for each atom are listed in Table 8. These values were computed using the Busing *et al.* (1964) program ORFFE and the temperature-factor tensors, β_{ij}, listed in Table 4. This program was also used to compute rms displacements along interatomic vectors mentioned in the following discussion.

The equivalent isotropic temperature factors listed in Table 4 for Si, Al, and the oxygen atoms are comparable to previously determined values in well-refined, ordered structures (Burnham, 1965*b*). For Na there are at present very few reliable values in the literature; our value of 0.95 is comparable to that of 1.10 found for Na in pectolite (Prewitt, 1965). The rms displacements listed in Table 8 show that the apparent thermal vibrations of all atoms except Al are significantly anisotropic. The most noteworthy, and indeed perplexing, feature is the small displacement (0.035±0.016 Å) of O_1 along axis r_1.

The orientation of the ellipsoid for O_1 is such that the rms displacements of O_1 toward its coordinating cations are 0.081 Å (±0.007 Å) toward Na, 0.039 Å (±0.014 Å) toward Si, and 0.069 and 0.072 Å (both ±0.008 Å) toward the two Al atoms. If we were dealing with a relatively simple case of harmonic vibration due to thermal energy alone, we would expect the vibration amplitude to be inversely proportional to bond strength; such is not the case, however, since the Si-O_1 bond is the longest Si-O bond and the Na-O_1 bond is the shortest Na-O bond. We see roughly the same situation with O_3. Here the rms displacements toward the two Si to which it is coordinated are both 0.077 Å (±0.008 Å), but the rms displacement toward the Na at 2.741 Å is 0.072 Å (±0.008 Å), whereas

that toward the Na at 2.363 Å is 0.088 Å (±0.007 Å). The displacements of O_2 toward its coordinating cations are more uniform, with differences less than 1σ. This is perhaps related to the deficiency of electrostatic charge on O_2 as opposed to the surplus on both O_1 and O_3.

Turning now to the rms displacements of Si and Na toward their coordinating anions, the general relations are opposite from what we might expect. The Si displacements toward O_1 and both O_3's are all 0.070 Å

TABLE 8. MAGNITUDE AND ORIENTATIONS OF PRINCIPAL AXES OF THERMAL ELLIPSOIDS

Atom, axis	rms displacement, Å, (σ)	Angle (°) with respect to:		
		$+a$ ($\pm\sigma$)	$+b$ ($\pm\sigma$)	$+c^*$ ($\pm\sigma$)
Na, r_1	0.089 (5)	69±4	90	21±4
r_2	0.097 (5)	90	0	90
r_3	0.136 (4)	21±4	90	111±4
Al, r_1	0.066 (6)	82±29	90	8±29
r_2	0.074 (6)	90	0	90
r_3	0.074 (6)	8±29	90	98±29
Si, r_1	0.067 (4)	107±16	85±11	18±8
r_2	0.068 (4)	163±16	92±20	107±15
r_3	0.080 (4)	90±9	5±9	95±9
O_1, r_1	0.035 (16)	33±14	75±8	61±14
r_2	0.067 (9)	58±15	99±13	147±14
r_3	0.090 (7)	98±9	18±9	106±12
O_2, r_1	0.056 (9)	36±11	72±12	60±15
r_2	0.079 (7)	104±17	127±19	40±18
r_3	0.094 (7)	122±11	42±18	66±17
O_3, r_1	0.067 (9)	35±53	78±17	122±61
r_2	0.073 (8)	120±58	101±20	148±61
r_3	0.093 (6)	106±13	16±14	93±13

(within 1σ), whereas that toward O_2 (1.590 Å away) is 0.078 Å (±0.004 Å). The Na displacement toward O_1 (along the shortest Na-O vector) is 0.112 Å (±0.003 Å), whereas that toward O_2 is 0.090 Å (±0.005 Å). Only the displacements of Na toward the two coordinating O_3 atoms bear the expected relationship: 0.096 Å (±0.004 Å) toward O_3 at 2.363 Å and 0.122 Å (±0.003 Å) toward O_3 at 2.741 Å.

These thermal models present a confusing picture, and since there are at present so few reliable data on which to base a comparison, a physical interpretation is virtually impossible. One likely explanation for the rela-

tively larger displacements of O_1 and O_3 toward Na along the shorter bonds is found by analogy to thermal data on disordered structures, namely that these displacements are non-thermal and are due to the presence of small amounts of Ca (Table 1) in the Na site.

We are still left with no explanation for the small displacement of O_1 toward Si and the relatively large displacement of Si toward O_2. The decision as to whether these are, in fact, real anomalies must be postponed until additional data from other precise refinements of diopside-type pyroxenes become available.

Comments on Structural Stability

For many years it was thought that jadeite was stable only at high pressure (Yoder, 1950), but today it is known that high pressure is required for synthesis at temperatures where reactions take place and that jadeite is probably quite close to, if not in, its stability field at room temperature and pressure. When temperature is raised at atmospheric pressure jadeite breaks down to albite plus nepheline, *i.e.*,

$$2NaAlSi_2O_6 \rightarrow NaAlSi_3O_8 + NaAlSiO_4$$

At room temperature and pressure the combined cell volumes of albite and nepheline are 22 per cent larger than twice the jadeite cell volume. This change in volume is a reflection of structural changes because in jadeite the aluminum coordination is 6 and in the others, 4. Sodium coordination is roughly the same in all three structures, but the average Na-O distance is about 6 per cent shorter in jadeite than in the other two.

It would be of interest to find some criterion for stability of a structure under changing conditions of temperature and pressure. This would be, for example, an interatomic distance which, when extended or compressed beyond some limit, would result in instability. Such analysis of silicates is difficult at present because little is known about how these structures, determined at room temperature and pressure, may differ from the actual structures which exist when the phases are formed.

Acknowledgments

We thank Dr. H. S. Yoder, Jr., for providing the sample used in this study and Professor C. E. Tilley for examining the optical properties of our specimen. Professor J. V. Smith kindly provided us with the detailed microprobe analysis of both the bulk sample and the single crystal used for intensity measurements. We also thank Drs. J. R. Clark, G. V. Gibbs, J. J. Papike, and D. R. Peacor for reviewing the manuscript and providing numerous suggestions for its improvement.

Appendix

Weighting. Observed structure factors were weighted in inverse proportion to their variance for least-squares refinement. Estimates

$$\left(w_{|Fo|} = \frac{1}{\sigma^2_{|Fo|}}\right)$$

of $\sigma_{|Fo|}$ based primarily on counting statistics were obtained using the following relation:

$$\sigma_{|Fo|} = \frac{|F_o|}{2I}\left[E + \frac{T_e}{2T_b}B + (0.03I)_2\right]^{1/2} \tag{A.1}$$

Here E is the total counts (peak+background) accumulated during continuous ω scan of the reflection profile; B is the total background computed according to

$$B = T_e\left(\frac{B_1 + B_2}{2T_b}\right) \tag{A.2}$$

where B_1 and B_2 are fixed-time background counts on each side of the peak; T_e is the time taken to scan the peak; and T_b is the fixed time for counting each background. The term $(0.03I)^2$ allows for miscellaneous, otherwise unaccounted for, fluctuations.

Intensities were considered to be below the minimum observable if

$$(E - 0.6745\sigma_E) - (B + 0.6745\sigma_B) < 0 \tag{A.3}$$

For those reflections satisfying (A.3) the value of $I_{\min.}$ was computed using (A.3) as an equality.

Scattering factors. In our least-squares refinement program scattering factors were computed using the expression (Silverman and Simonsen, 1960; Fischer, 1963):

$$f_i = \exp\left[\sum_{n=0}^{6} a_n (\sin\theta/\lambda)^n\right] \tag{A.4}$$

The least-squares program was provided with one set of constants a_{0i} through a_{6i} for each kind of atom. The constants were determined by the following method, the basic features of which were suggested to us by Fischer (personal communications, 1961–1963): The f values for a particular atom are obtained from tables, curves are drawn, and additional f values are interpolated for intermediate values of $\sin\theta/\lambda$. These are used in a least-squares refinement in which the f values are treated as a set of $|F_o|$. These are compared with f values calculated using the constants a_i for a one-atom structure with the atom at the origin of the unit cell. Consecutive indices $h00$ are assigned each "observation" which, with appropriate choice of lattice constant, represent $\sin\theta/\lambda$ increments of 0.025. Since a_o, by definition, is equal to ln Z, where Z is the number of electrons, the value of a_o is fixed by the ionization state of the atom, and is not varied. The best values of a_1 through a_6 are determined by several cycles of least-squares refinement of the fictitious structure. In all cases the f values calculated using the refined values of the a_i agree very well with the "observed" values. The constants a_i for fully ionized atoms, valid in the range $0 \leqq \sin\theta/\lambda \leqq 1.3$, are given below.

Na^{1+}	2.30259	0.02175	−5.02831	1.88387	4.68622	−4.37294	1.98615
Al^{3+}	2.30259	−0.00332	−2.60085	−0.48861	3.32426	−2.12639	0.43425
Si^{4+}	2.30259	−0.00269	−2.10046	−0.10831	1.44082	−0.56796	0.02120
O^{2-}	2.30259	0.10528	−23.00186	58.47558	−64.85647	34.48609	−7.19208

The "observed" f values for all atoms, both neutral and ionized, with the exception of O^{2-}, were taken from the *International Tables for X-ray Crystallography*, vol. III, pp. 202–203 (1962). Those for O^{2-} were given by Suzuki (1960).

Anomalous dispersion corrections. Anomalous dispersion coefficients, Δf_r and Δf_i were taken from *International Tables for X-ray Crystallography*, vol. III, p. 214 (1962). When these corrections are included, structure factors for centric crystals such as jadeite are calculated according to

$$F_c = [A_r^2 + A_i^2]^{1/2} \tag{A.5}$$

where

$$\begin{aligned} A_r &= \sum (f + \Delta f_r)\xi \cos\phi \\ A_i &= \sum \Delta f_i \xi \cos\phi \end{aligned} \tag{A.6}$$

and ξ and ϕ are scale and temperature factors and trigonometric parts of the structure factors.

References

Buerger, M. J. and C. T. Prewitt (1961) The crystal structures of wollastonite and pectolite. *Proc. Nat. Acad. Sci.* **47,** 1883–1888.

Burnham, Charles W. (1962) Lattice constant refinement. *Carnegie Inst. Wash. Year Book* **61,** 132–135.

——— (1963) Refinement of the crystal structure of kyanite. *Zeit. Krist.* **118,** 337–360.

——— (1965a) Computation of absorption corrections, and the significance of end effect. *Am. Mineral.* **50,** in press.

——— (1965b) Temperature parameters of silicate crystal structures (abstract). *Am. Mineral.* **50,** 282.

Busing, W. R., K. O. Martin and H. A. Levy (1964) ORFFE, a FORTRAN crystallographic function and error program. Oak Ridge National Laboratory, Oak Ridge, Tennessee.

Clark, S. P., Jr., J. F. Schairer and J. de Neufville (1962) Phase relations in the system $CaMgSi_2O_6$-$CaAl_2SiO_6$-SiO_2 at low and high pressure. *Carnegie Inst. Wash. Year Book* **61,** 59–68.

Coleman, R. G. (1961) Jadeite deposits of the Clear Creek Area, New Idria District, San Benito County, California. *Jour. Petrol.* **2,** 209–247.

Cruickshank, D. W. J. (1960) *Computing Methods and the Phase Problem in X-Ray Crystal Analysis*, edited by Ray Pepinsky, J. M. Robertson and J. C. Speakman. Pergamon Press, London.

Deer, W. A., R. A. Howie and J. Zussman (1963) *Rock-Forming Minerals*, Vol. II, John Wiley and Sons, Inc., New York.

Fischer, K. (1963) Least-squares refinement of atomic scattering factors: possibilities, techniques, and applications, Abstracts of ACA Annual Meeting, Cambridge, Mass., p. 41.

Frondel, C. and C. Klein, Jr. (1965) Ureyite, $NaCrSi_2O_6$: A new meteoritic pyroxene. *Science* **149,** 742–744.

Hamilton, W. C. (1955) On the treatment of unobserved reflexions in the least-squares adjustment of crystal structures. *Acta Cryst.* **8,** 185–186.

——— (1959) On the isotropic temperature factor equivalent to a given anisotropic temperature factor. *Acta Cryst.* **12,** 606–610.

Kuno, H. and H. H. Hess (1953) Unit cell dimensions of clinoenstatite and pigeonite in relation to the common pyroxenes. *Am. Jour. Sci.*, **251,** 741–752.

Morimoto, Nobuo, D. E. Appleman and H. T. Evans, Jr. (1960) The crystal structures of clinoenstatite and pigeonite. *Zeit Krist.* **114,** 120–147.

Pauling, Linus (1960) *The Nature of the Chemical Bond*, 3rd ed., Cornell University Press, Ithaca, N. Y.

Prewitt, C. T. (1962) Unpublished least-squares computer program.

——— (1964) Crystal structures of two synthetic amphiboles (abs.). *Geol. Soc. Am. Spec. Paper* **76,** 132.

——— (1965) Refinement of pectolite. In preparation.

Silverman J. and S. Simonsen (1960) A useful analytic approximation to atomic and unitary atomic scattering factors. *Acta Cryst.* **13,** 50–55.

Suzuki, T. (1960) Atomic scattering factor for O^{2-}. *Acta Cryst.* **13,** 279.

Warren, B. E. and J. Biscoe (1931) The crystal structure of the monoclinic pyroxenes. *Zeit Krist.* **80,** 391–401.

Warren, B. E. and W. L. Bragg (1928) The structure of diopside $CaMg(SiO_3)_2$. *Zeit Krist.* **69,** 168–193.

Wyckoff, R. W. G., H. E. Merwin and H. S. Washington (1925) *X*-ray diffraction measurements upon the pyroxenes. *Am. Jour. Sci.* **10,** 383–397.

Yoder, Hatten S., Jr., (1950) The jadeite problem. *Am. Jour. Sci.* **248,** 225–248, 312–334.

——— and C. W. Chesterman (1951) Jadeite of San Benito County, California. *Calif. Div. Mines Spec. Report* **10-C,** 1–8.

Zacharaisen, W. H. (1963) The crystal structure of cubic metaboric acid. *Acta Cryst.* **16,** 380–384.

Manuscript received, December 3, 1965; accepted for publication, December 14, 1965.

TOPS FORM 3616
SITHO IN U.S.A.

Santa Rita Rock Jadeite

	UCLA	CIT	STOICH	AVG
WT %				
SiO_2	57.56	59.55	59.46	59.50
TiO_2	0.00	0.00	—	—
Al_2O_3	25.18	25.11	25.21	25.17
FeO	0.05	0.05	—	0.05
CaO	0.05	0.07	—	0.06
MgO	0.00	0.01	—	0.03
Na_2O	15.45	15.37	15.33	15.32
K_2O	0.00	0.00	—	—
F.P.'s (4)				
Si	.99126	1.997	.99109	2.002	.98960	2.000
Ti	—		—		—	
Al	.49391	0.995	.49253	0.995	.49449	1.000
Fe	.00070	0.001	.00070	0.001	—	
Ca	.00089	0.002	.00175	0.002	—	
Mg	—		.00025	0.001	—	
Na	.49856	1.004	.49436	0.999	.49468	1.000
K	—		—		—	
Si	.99026	1.9997				
Al	.49371	0.9970				
Fe	.00070	0.0014				
Ca	.00107	0.0022				
Mg	.00074	0.0015				
Na	.49436	0.998				

3 June 82 MBX
DEZ

Jadeite $NaAlSi_2O_6$

assume 0.20 FeO = 0.22 Fe_2O_3 0.10 CaO

$Ca_2Si_2O_6$

100.00			
− .21	$Ca_2Si_2O_6$	56.08	.16
		60.08	.11
		116.16	
99.79			
− .64	$NaFeSi_2O_6$	79.84	.22
		30.99	.09
		60.08	.33
		60.08	
99.15	$NaAlSi_2O_6$	230.99	

30.99	
50.98	
120.16	
202.13	

	SiO_2	Na_2O	Al_2O_3	Fe_2O_3	CaO
$NaAlSi_2O_6$	58.94	15.20	25.01		
$NaFeSi_2O_6$	.33	.09		.22	
$Ca_2Si_2O_6$	.11				.10
	59.38	15.29	25.01	.22	.10

	This work		UCLA	CIT	STOICH	ARL Probe
SiO_2	(59.4)	Calculated on STOICH	59.56	59.55	59.46	
Al_2O_3	(25.0)		25.18	25.11	25.17	
Na_2O	(15.3)		15.45	15.32	15.33	
FeO	.2		.05	.05	–	.15
CaO	.1		.05	.07	–	.10
MgO	0		00	.01	–	.03
MnO	0				–	.00
TiO_2	.04				–	.03

NATIONAL
12-383
Made in U.S.A.

SANTA RITA PEAK JADEITE

	Na_2O	MgO	Al_2O_3	SiO_2	CaO	TiO_2	K_2O	MnO	FeO	Fe_2O_3
	(BLUE FLUOR)									
PROBE	16.62	0.01	24.89	58.07	0.14	0.05-0.10	0.04	—	—	0.43
J.V.	(TURQUOISE FLUOR)									
Smith	16.44	0.46	24.59	57.68	0.87	0.00-0.03	0.02	0.03-0.05	—	0.50
	↑			↑						
	High			Low	(bad stoichiometry)					
WET CHEM	14.95	0.17	24.62	59.06	0.35	0.08	0.01	0.03	0.18	0.41